Computational Materials Science 45 (2009) 511–515

Contents lists available at ScienceDirect

Computational Materials Science

journal homepage: www.elsevier.com/locate/commatsci

Identification of elastic constants of FCC metals from 2D load-indentation curves

W. Jiang, R.C. Batra *

Department of Engineering Science and Mechanics, Virginia Polytechnic Institute and State University, M/C 0219, Blacksburg, VA 24061, United States

ARTICLE INFO

Article history:
Received 18 March 2008
Received in revised form 25 October 2008
Accepted 25 November 2008
Available online 8 January 2009

PACS:
61.66.Bi
81.07.Lk

Keywords:
FCC material
Indentation load vs. indentation depth relation

ABSTRACT

We derive an expression relating the axial load, the indentation depth, and the elastic constants of an orthotropic material, and simplify it to that for a cubic material (e.g., an FCC single crystal). We use this formula and results of three virtual (i.e., numerical) indentation tests on the same specimen oriented differently to find values of the elastic moduli, and show that they agree well with their expected values. We also give the error in the computed values of the elastic moduli of an FCC crystal caused by the misorientation of the specimen during the indentation test. The technique can be generalized to other anisotropic materials.

1. Introduction

Very promising engineering applications of nanocomposites and nanofilms in miniaturized components have aroused considerable interest in finding mechanical properties of these materials. A commonly used mechanical test for determining elastic moduli of a material is the indentation test. With continuous improvements in accurately measuring very small loads and indentation depths, the technique is being applied to nano-materials which are generally anisotropic. An interpretation of test results and the extraction of material moduli are facilitated by analytical expressions relating the indentation load and the indentation depth. For anisotropic materials one needs to ascertain values of more than one elastic constant. Thus either different types of tests (e.g., tension, torsion etc.) or similar tests on different orientations of the specimen are needed to find values of the elastic moduli.

Analytical solutions of even linear three-dimensional (3D) boundary-value problems for elastic bodies are hard to find. Even though solutions in the form of infinite series (or finite series with a large number of terms) for some 3D boundary-value problems are available, they are not easily applicable to test data. A possibility is to use specimen geometries and test configurations so that deformations induced can be approximated as either plane strain or plane stress. The former (latter) is usually applicable when the specimen dimension in the axial direction is very large (small) as compared to the other two lateral dimensions, and the applied loads and the specimen geometry are independent of the axial coordinate. Here we study indentation problems when deformations of the indented body can be approximated as plane strain, and the indenter can be regarded as rigid. Thus elastic constants of the indenter material are very large as compared to those of the material being tested. Furthermore, by restricting indentation depths to very small values as compared to the smallest dimension of the specimen, one can use solutions for the half-space to interpret test results.

Doerner and Nix [5] and Oliver and Pharr [12] have analyzed infinitesimal deformations of a half-space indented by a flat punch, and a paraboloid indenter, respectively. The Oliver and Pharr [12] solution has been widely adopted to determine the elastic modulus of the material from results of indentation tests on nanosize specimens. Doerner and Nix [5] have given an empirical relation to account for the compliance of the substrate to which the specimen is perfectly bonded. The deformations of the substrate are usually considered when the indentation depth exceeds about 30% of the film thickness. Bhattacharya and Nix [3,4], used the finite element method to study elasto-plastic deformations during submicron scale indentations by conical indenters of a thin film bonded to a substrate. They developed empirical equations to determine the hardness for both hard-film/soft-substrate and soft-film/hard-substrate systems. Huber and Tsakmakis [7], and Huber et al. [8] used neural networks, trained by results of the finite element simulations of nanoindentation, to identify values of elastic-plastic and visco-plastic material parameters.

We note that Vlassak and Nix [17] have provided an expression for the indentation modulus of an anisotropic solid, and have used

* Corresponding author. Tel.: +1 540 231 6051; fax: +1 540 231 4574.
E-mail addresses: wjiang@vt.edu (W. Jiang), rbatra@vt.edu (R.C. Batra).

0927-0256/$ - see front matter © 2008 Elsevier B.V. All rights reserved.
doi:10.1016/j.commatsci.2008.11.015

it to interpret results of indentation experiments. By changing the orientation of the specimen, they found values of more than one elastic constant of the material. However, an examination of the indentation load vs. the indentation depth plots does not reveal an explicit correlation between the experimental data and the elastic moduli of anisotropic materials. Therefore, an inverse method is needed to extract values of material elasticities through suitable post-processing of the test data. Depending upon the number of independent elastic constants for an anisotropic material, the inverse process can be quite complicated. Sasaki et al. [13] combined the finite element simulation results of nanoindentation tests with an optimization technique to determine five material parameters of a transversely isotropic material.

Here we focus on finding values of three elastic constants of a face centered cubic (FCC) material such as gold, copper, and aluminum. By assuming that the specimen can be modeled as a half-space and its deformations as plane strain, we first derive an expression for the axial load in terms of elastic constants of the specimen material and the indentation depth. This relationship and results of three indentation tests for different orientations of the specimen enable us to find values of the three elastic constants. We also quantify the error in values of elastic moduli caused by misorientation of the specimen during an indentation test.

2. Load-displacement relation for an anisotropic half-space indented by a rigid circular cylinder

Fan and Hwu [6] and Hwu and Fan [10] have used the Eshelby-Stroh formalism to analyze a 2D generalized plane strain contact problem in which a long parabolic cylinder indents a linear elastic, anisotropic and homogeneous half-space. They found the stress distribution on the contact surface, and did not provide an explicit relation between the axial load P and the indentation depth u_0. We derive here such a relation.

A schematic sketch of the contact problem studied here is shown in Fig. 1. In rectangular Cartesian coordinates, equations governing generalized plane strain deformations of the half-space are

$$\sigma_{ij,j} = 0, \tag{1}$$

$$\sigma_{ij} = C_{ijkl}u_{k,l}, \tag{2}$$

$$C_{ijkl} = C_{jikl} = C_{ijlk} = C_{klij}. \tag{3}$$

Here σ_{ij} is the Cauchy stress tensor, C_{ijkl} an elastic constant of the material of the half-space, a comma followed by index j indicates partial differentiation with respect to the position x_j of a material point, and a repeated index implies summation over the range of the index. The length of the cylinder in the x_2 -direction is large as compared to its diameter, the contact width, and the indentation depth. Hence a generalized plane strain state of deformation in the x_1x_3 -plane is considered in the sense that all three displacement components and the six stress components induced are presumed not to depend upon x_3.

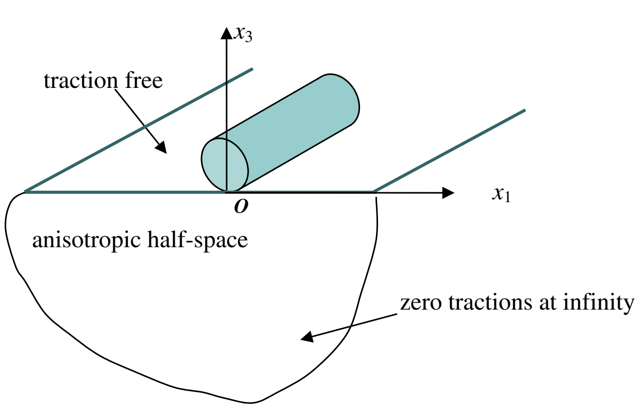

Fig. 1. Schematic sketch of the indentation of an anisotropic half-space by a rigid circular cylinder.

Using Stroh's formalism [14,15], we can write a general solution of Eqs. (1)–(3) as

$$\mathbf{u} = \mathbf{Af}(z) + \overline{\mathbf{Af}(z)}, \tag{4.1}$$

$$\Phi = \mathbf{Bf}(z) + \overline{\mathbf{Bf}(z)}, \tag{4.2}$$

where $\mathbf{A} = [\mathbf{a}_1\mathbf{a}_2\mathbf{a}_3]$, $\mathbf{B} = [\mathbf{b}_1\mathbf{b}_2\mathbf{b}_3]$, $\mathbf{f}(z) = [f_1(z_1), f_2(z_2), f_3(z_3)]^{\mathrm{T}}$, $z_\alpha = x_1 + p_\alpha x_2$, an overbar over a variable represents its complex conjugate, the superscript T denotes the transpose, and p_α, $(\mathbf{a}_\alpha, \mathbf{b}_\alpha)$ (α = 1,2,3) are eigenvalues and eigenvectors of the fundamental elasticity matrix $\mathbf{N}$. That is,

$$\mathbf{N}\zeta = p\zeta, \tag{5.1}$$

where $\zeta = (\mathbf{a},\mathbf{b})$ is an eigenvector of the matrix $\mathbf{N}$ with eigenvalue p,

$$\mathbf{N} = \begin{bmatrix} -\mathbf{T}^{-1}\mathbf{R}^{\mathrm{T}} & \mathbf{T}^{-1} \\ \mathbf{RT}^{-1}\mathbf{R}^{\mathrm{T}} - \mathbf{Q} & -\mathbf{RT}^{-1} \end{bmatrix} \tag{5.2}$$

and $Q_{ik} = C_{i1k1} = Q_{ki}$, $R_{ik} = C_{i1k3}$ and $T_{ik} = C_{i3k3} = T_{ki}$ are 3×3 matrices. The function $\mathbf{u}$ represents displacements, and the function $\mathbf{\Phi}$ serves as a potential for stresses. That is

$$\sigma_{i1} = -\phi_{i,3} \tag{6.1}$$

$$\sigma_{i3} = \phi_{i,1} \qquad i = 1, 3. \tag{6.2}$$

The holomorphic complex valued function $\mathbf{f}(z)$ is to be determined by satisfying the equilibrium Eq. (1) and the prescribed boundary conditions.

When the indentation depth u_0 is small as compared to the radius R of the circular cylindrical indenter, the profile of the indenter in the vicinity of the contact point $(0,-u_0)$ in Fig. 1 can be approximated as parabolic. The pressure on the contact surface between a smooth rigid parabolic indenter $x_3 = x_1^2/2R$, and a homogeneous anisotropic half-space is given by (e.g., see Hwu and Fan [10], Hwu [9])

$$\sigma_{33} = -\frac{1}{\beta R}\sqrt{a^2 - x_1^2}, \qquad |x_1| < a, \tag{7}$$

where contact extends from $x_1 = -a$ to $x_1 = a$, $\beta = (M^{-1})_{33}$, and $\mathbf{M}^{-1} = i\mathbf{AB}^{-1}$. Since the matrix $\mathbf{M}$ is Hermitian [16], i.e., $\mathbf{M} = \bar{\mathbf{M}}^{\mathrm{T}}$, $(M^{-1})_{33}$ is a real number. For an orthotropic material

$$\frac{1}{\beta} = \frac{1}{(M^{-1})_{33}} = \sqrt{\frac{C_{55}(\sqrt{C_{11}C_{33}} - C_{13})}{C_{11}(C_{13} + 2C_{55} + \sqrt{C_{11}C_{33}})}}\left(C_{13} + \sqrt{C_{11}C_{33}}\right) \tag{8}$$

Here C_{ij} is an elastic constant of the orthotropic half-space in the contracted notation in which the stress and the strain tensors are written as six dimensional vectors, and the 4th order elasticity tensor C_{ijkl} as a 6×6 symmetric matrix. The correspondence between C_{ij} and C_{ijkl} is given in many books, e.g., see Batra [2].

Barnett and Lothe [1] and Ting [16] have given the following expression for the displacement field in an orthotropic half-space due to a line force $\mathbf{f} = -[f_1 \quad f_2 \quad f_3]^{\mathrm{T}}$.

$$\mathbf{u} = \frac{1}{\pi}\mathrm{Im}\{\mathbf{A}\langle \ln z_* \rangle \mathbf{B}^{-1}\mathbf{f}\}, \tag{9}$$

where $\langle \ln z_* \rangle = \mathrm{diag}[\ln z_1, \ln z_2, \ln z_3]$. For a line load only in the vertical direction, i.e., (f_1=f_2=0), Eq. (9) gives the following expression for the vertical displacement of a point of the half-space

$$u_3 = -\frac{f_3}{\pi}\mathrm{Im}[A_{31}(B^{-1})_{13}\ln z_1 + A_{32}(B^{-1})_{23}\ln z_2 + A_{33}(B^{-1})_{33}\ln z_3]. \tag{10}$$

Thus for a point on the vertical axis

$$\begin{aligned} u_3(x_1, 0) &= -\frac{f_3}{\pi}\mathrm{Im}[A_{31}(B^{-1})_{13} + A_{32}(B^{-1})_{23} + A_{33}(B^{-1})_{33}]\ln x \\ &= \frac{f_3(M^{-1})_{33}}{\pi}\ln x. \end{aligned} \tag{11}$$

For the present contact problem, the displacement of a point on the vertical axis can be computed from Eq. (11) by setting $f_3 = \sigma_{33}ds$ and integrating the right-hand side of the resulting equation from $-a$ to $+a$. The result is

$$u_3(x,0) = -\frac{(M^{-1})_{33}}{\pi}\int_{-a}^{a}\sigma_{33}(s)\ln|x-s|ds. \tag{12}$$

Substituting for σ_{33} from Eq. (7) into Eq. (12), we obtain

$$u_3(x,0) = \frac{1}{\pi R}\int_{-a}^{a}\sqrt{a^2-s^2}\ln|x-s|ds. \tag{13}$$

Noting that Eq. (13) has been derived without using any displacement type boundary condition, we remove the rigid body translation by measuring the vertical displacement of a point relative to that of a reference point $(x_0,0)$; e.g., see Johnson [11, p.17]. Thus

$$\begin{aligned} u_3'(x_1,0) &= u_3(x_1,0) - u_3(x_0,0) \\ &= \frac{1}{\pi R}\int_{-a}^{a}\sqrt{a^2-s^2}\ln\left|\frac{x_1-s}{x_0-s}\right|ds, \end{aligned} \tag{14}$$

$u_3'(x_0,0) = 0$, and the prime indicates the displacement of a point relative to that of the point $(x_0,0)$. We choose the reference point on the free surface of the half-space and far from the contact area, i.e., $x_1 \gg a$.

The indentation depth u_0 can be computed from

$$\begin{aligned} u_0 &= -u_3(0,0) + u_3(x_0,0) = -\frac{1}{\pi R}\int_{-a}^{a}\sqrt{a^2-s^2}\ln\frac{|s|}{x_0-s}ds \\ &= \frac{a^2}{2R}[-\ln a + \ln(2x_0\sqrt{e})] + O\left(\frac{1}{x_0^2}\right) \end{aligned} \tag{15}$$

Also, the axial load P per unit length of the indenter found by integrating Eq. (7) over the contact width is given by

$$P = \int_{-a}^{a}\sigma_{33}(x_1,0)dx_1 = \frac{\pi a^2}{2\beta R}. \tag{16}$$

Solving Eq. (16) for a and substituting for a in Eq. (15), we obtain the following load-displacement relation for the indentation problem:

$$-\frac{1}{\beta}\frac{\pi u_0}{P} = \ln\sqrt{P} - \ln\sqrt{P_0}, \tag{17}$$

where $P_0 = \frac{2\pi e x_0^2}{\beta R}$.

3. Determination of elasticities of an FCC material

3.1. Method

An FCC single crystal has three independent elastic constants. With lattice directions [100], [010] and [001] aligned along the rectangular Cartesian coordinate axes, the 6×6 matrix $\mathbf{C}$ of elasticities has the form:

$$\mathbf{C} = \begin{bmatrix} C_{11} & C_{12} & C_{12} & 0 & 0 & 0 \\ C_{12} & C_{11} & C_{12} & 0 & 0 & 0 \\ C_{12} & C_{12} & C_{11} & 0 & 0 & 0 \\ 0 & 0 & 0 & C_{44} & 0 & 0 \\ 0 & 0 & 0 & 0 & C_{44} & 0 \\ 0 & 0 & 0 & 0 & 0 & C_{44} \end{bmatrix} \tag{18}$$

With respect to rectangular Cartesian coordinate axes $x_i'(i=1,2,3)$ obtained by rotating axes x_j with the matrix $\mathbf{a}$ given by

$$\mathbf{a} = \begin{bmatrix} a_{11} & a_{12} & a_{13} \\ a_{21} & a_{22} & a_{23} \\ a_{31} & a_{32} & a_{33} \end{bmatrix}, \tag{19}$$

where a_{ij} equals cosine of the angle between x_i' and x_j, the matrix $\mathbf{C}'$ of elasticities is related to the matrix $\mathbf{C}$ by

$$\mathbf{C}' = \mathbf{QC}\bar{\mathbf{Q}}^{-1} \tag{20}$$

where elements of matrices $\mathbf{Q}$ and $\bar{\mathbf{Q}}$ in terms of those of matrix $\mathbf{a}$ are given in Batra [2].

As shown in Fig. 2, besides the x_j- axes, we consider three sets of rectangular Cartesian coordinate axes x_i', namely, those obtained by rotating the coordinate axes x_j through $-45°$ about the x_1- axis, the x_2- axis, and the x_3- axis. Values of $1/\beta$ with respect to these four sets of coordinate axes are denoted below by $(1/\beta)_{\text{I}}$, $(1/\beta)_{\text{II}}$, $(1/\beta)_{\text{III}}$, and $(1/\beta)_{\text{IV}}$, respectively; their values in terms of elements of the matrix $\mathbf{C}$ are given below as Eqs. (21):

$$\left(\frac{1}{\beta}\right)_{\text{I}} = \left(\frac{1}{\beta}\right)_{\text{III}} = \sqrt{\frac{C_{44}(C_{11}-C_{12})}{C_{11}\gamma}}(C_{12}+C_{11}) \tag{21.1}$$

$$\left(\frac{1}{\beta}\right)_{\text{II}} = \sqrt{\frac{C_{44}(\sqrt{C_{11}\gamma/2}-C_{12})}{C_{11}(C_{12}+2C_{44}+\sqrt{C_{11}\gamma/2})}}\left(C_{12}+\sqrt{C_{11}\gamma/2}\right) \tag{21.2}$$

$$\left(\frac{1}{\beta}\right)_{\text{IV}} = \sqrt{\frac{2C_{44}(\sqrt{C_{11}\gamma/2}-C_{12})}{\gamma(C_{12}+2C_{44}+\sqrt{C_{11}\gamma/2})}}\left(C_{12}+\sqrt{C_{11}\gamma/2}\right) \tag{21.3}$$

$$\gamma = C_{12}+2C_{44}+C_{11} \tag{21.4}$$

By dividing each side of Eq. (21.3) by the corresponding side of Eq. (21.2), we obtain

$$\left(\frac{1}{\beta}\right)_{\text{IV}}\bigg/\left(\frac{1}{\beta}\right)_{\text{II}} = \sqrt{\frac{2}{\gamma}}. \tag{23}$$

The three unknowns C_{11}, C_{12}, and C_{44} can be determined in terms of $(1/\beta)_{\text{I}}$ or $(1/\beta)_{\text{III}}$, $(1/\beta)_{\text{II}}$, and $(1/\beta)_{\text{IV}}$ by simultaneously solving Eqs. (21.1), (21.2), and (21.3).

We propose the following procedure for finding the three elastic constants of an FCC material. Perform indentation tests on a sample of the material with lattice vectors coincident with the three sets of coordinate axes x_i' given above, and find the corresponding values of $(1/\beta)$ by using slopes of the axial load vs. indentation

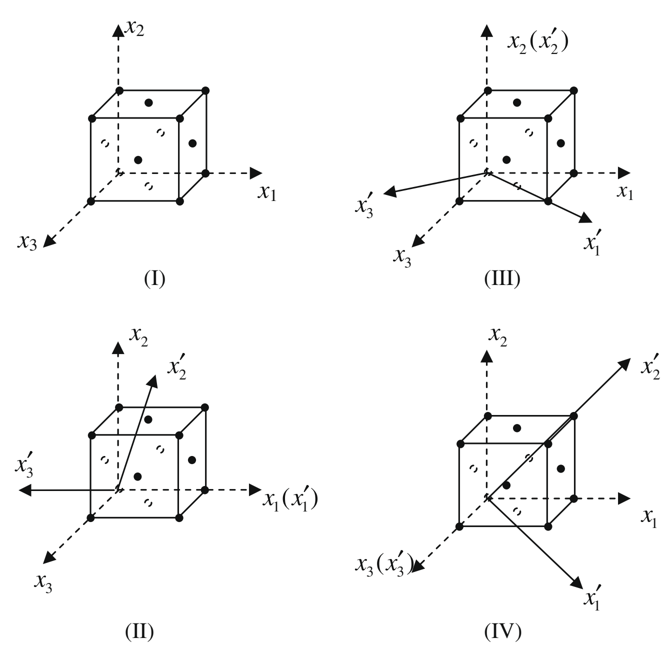

Fig. 2. (I) Rectangular Cartesian coordinate axes x_j aligned with the lattice directions [100], [010] and [001]; (II)–(IV) rectangular Cartesian coordinate axes x_i' obtained by rotating axes x_j through $-45°$ about the x_1 -axis, the x_2 -axis and the x_3 -axis, respectively.

curves and Eq. (17). Then solve simultaneously Eqs. (21.1), (21.2), and (21.3) for C_{11}, C_{12} and C_{44}.

3.2. Application of the method

We use the proposed method to find three elastic constants of a single crystal of gold. We perform four virtual (i.e., numerical) indentation tests on a gold crystal of dimensions 204 Å × 102 Å with lattice vectors oriented as stated above in Section 3.1. The radius of the cylinder is taken to be 40 Å. The bottom surface of the layer is kept fixed, the left and the right surfaces are traction free, and the top surface is indented with a parabolic indenter. During all simulations, the indentation is kept less than 10.2 Å, (i.e., 10% of the height of the specimen) and the contact width less than 20 Å (i.e., less than 10% of the specimen width). These constraints should minimize the effect of boundary conditions on the left and the right surfaces, and ensure that the relation (17) between the axial load and the indentation depth for the half-space derived in Section 2 is valid.

We assume that a gold crystal can be modeled as a continuum, and plot results of our virtual tests in the form of the indentation load vs. the indentation depth curves as shown in Fig. 3. Eq. (17) implies that the plot of $\ln\sqrt{P}$ vs. $\pi u_0/P$ should be a straight line. Accordingly, we fit straight lines by the least squares method to the data plotted in Fig. 3 and find slopes of the lines with the following results

$$\begin{aligned}
&(1/\beta)_{\mathrm{I}} = 40.1\mathrm{GPa}\\
&(1/\beta)_{\mathrm{II}} = 53.3\mathrm{GPa}\\
&(1/\beta)_{\mathrm{III}} = 41.0\mathrm{GPa}\\
&(1/\beta)_{\mathrm{IV}} = 49.0\mathrm{GPa}
\end{aligned} \tag{24}$$

Since results for tests 1 and 3 should be the same, we take average of values of $(1/\beta)_{\mathrm{I}}$ and $(1/\beta)_{\mathrm{III}}$, and set $(1/\beta)_{\mathrm{I}} = (1/\beta)_{\mathrm{III}} = 40.55$ GPa. Substitution from Eq. (24) into Eqs. (21.1)–(21.3) and solving simultaneously the three resulting equations, we get

$$C_{11} = 179.3\mathrm{GPa},\ C_{12} = 154.5\mathrm{GPa},\ C_{44} = 45.3\mathrm{GPa}$$

which differ by less than 3% from the values of C_{11}, C_{12} and C_{44} used as input into the code.

3.3. Effect of misorientation of the specimen

In a laboratory, there may be errors introduced in rotating the specimen through the desired angle. Accordingly, we conducted another set of numerical tests in which the angle of rotation was

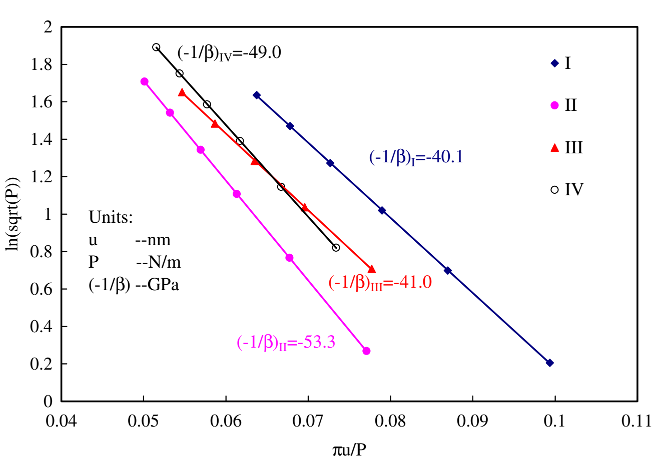

Fig. 3. Plot of the indentation load vs. the indentation depth for four virtual experiments on a gold crystal.

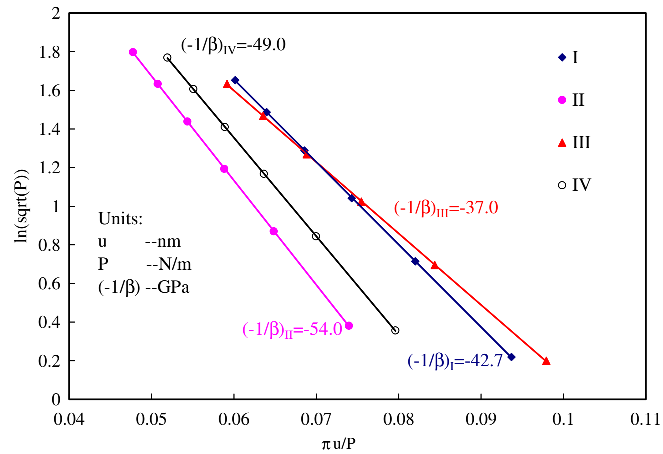

Fig. 4. Plot of the indentation load vs. the indentation depth for four virtual experiments on a gold crystal with specimens misoriented by less than 6°.

set randomly between -39° and -51°. Results of these simulations are depicted in Fig. 4, and values of material parameters determined from results of these simulations are $C_{11} = 166.1$ GPa, $C_{12} = 142.6$ GPa, $C_{44} = 47.4$ GPa, which differ from their values input into the code by less than 10.3%. Thus the misorientation of the crystal by 6° in the indentation tests can affect values of the three elastic constants by 10%.

3.4. Remarks

One possible difficulty in adopting the proposed procedure to physical experiments is to use a long cylindrical indenter. For commonly used conical and spherical indenters, deformations of the indented body can not be approximated as 2D. Whereas one can deduce the load-indentation plots through numerical experiments, the identification of material elasticities becomes an iterative process. For finding all three elastic constants of an FCC metal, the iterative process can become computationally expensive. The situation is further compounded if the lattice orientation cannot be determined a priori.

The proposed technique can also be applied to find elastic constants of materials of other symmetries. For example, one will need five (nine) suitably selected linearly independent orientations of the specimen for a transversely isotropic (an orthotropic) material so that all elastic constants appear at least once in the expression for the slope of the load vs. indentation curve. Since β given by Eq. (8) is a nonlinear function of the material elasticities, one will need to solve simultaneously a system of five or nine nonlinear algebraic equations to evaluate the material elasticities. If necessary, these equations can be solved by an iterative method.

4. Conclusions

We have developed an expression relating the axial load to the depth of indentation for plane strain deformations of an anisotropic half-space indented by a rigid parabolic indenter. This expression involves material elasticities. By using results of three indentation tests on a face centered cubic material with each test performed on a differently oriented specimen, we obtain three linearly independent equations for the three elastic constants. It is shown that when the indentation depth and the contact width are less than 10% of the thickness and the width of the thin layer of the specimen bonded to a relatively rigid substrate, then the proposed inverse method yields very good values of the three elastic constants of a face centered cubic material.

Acknowledgements

This work was partially supported by the ONR Grant N00014-06-1-0567 to Virginia Polytechnic Institute and State University with Dr. Y.D.S. Rajapakse as the program manager, and the Institute of Critical Sciences and Technology, VPI&SU. Views expressed in the paper are those of authors and neither of the funding agencies nor of VPI&SU.

References

[1] D.M. Barnett, J. Lothe, Line force loadings on anisotropic half-spaces and wedges, Physica Norvegica 8 (1975) 13–22.
[2] R.C. Batra, Elements of Continuum Mechanics, AIAA, Reston, 2005.
[3] A.K. Bhattacharya, W.D. Nix, Finite element simulation of indentation experiments, International Journal of Solids and Structures 24 (1998) 881–891.
[4] A.K. Bhattacharya, W.D. Nix, Analysis of elastic and plastic deformation associated with indentation testing of the thin films on substrates, International Journal of Solids and Structures 24 (1998) 1287–1298.
[5] M.F. Doerner, W.D. Nix, A method for interpreting the data from depth-sensing indentation instruments, Journal of Materials Research 1 (1986) 601–609.
[6] C.W. Fan, C. Hwu, Punch problems for anisotropic elastic half-plane, Journal of Applied Mechanics 63 (1996) 69–76.
[7] N. Huber, C. Tsakmakis, A neural network tool for identifying the material parameters of a finite deformation viscoplasticity model with static recovery, Computer Methods in Applied Mechanics and Engineering 191 (3–5) (2001) 353–384.
[8] N. Huber, W.D. Nix, H. Gao, Identification of elastic-plastic material parameters from pyramidal indentation of thin films, Proceedings of the Royal Society of London Series A-Mathematical Physical and Engineering Sciences 458 (2023) (2002) 1593–1620.
[9] C. Hwu, Fracture parameters for the orthotropic bimaterial interface cracks, Engineering Fracture Mechanics 45 (1) (1993) 89–97.
[10] C. Hwu, C.W. Fan, Sliding punches with or without friction along the surface of an anisotropic elastic half-plane, Quarterly Journal of Mechanics and Applied Mathematics 51 (1998) 159–177.
[11] K.L. Johnson, Contact Mechanics, Cambridge University Press, Cambridge, UK, 1985.
[12] W.C. Oliver, G.M. Pharr, An improved technique for determining hardness and elastic modulus using load and displacement during indentation experiments, Journal of Material Research 7 (1992) 1564–1583.
[13] T. Sasaki, M. Yang, S. Fukushima, R. Tsukano, Development of the CAE-assisted nano-indentation method for the evaluation of the anisotropic mechanical-properties of thin films, Journal of Material Processing and Technology 151 (2004) 263–267.
[14] A.N. Stroh, Dislocations and cracks in anisotropic elasticity, Philosophical Magazine 7 (1958) 625–646.
[15] A.N. Stroh, Steady state problems in anisotropic elasticity, Journal of Mathematics and Physics 41 (1962) 77–103.
[16] T.C.T. Ting, Effects of change of reference coordinates on the stress analyses of anisotropic elastic materials, International Journal of Solids and Structures 18 (1982) 139–152.
[17] J.J. Vlassak, W.D. Nix, Measuring the elastic properties of anisotropic materials by means of indentation experiments, Journal of the Mechanics and Physics of Solids 42 (1994) 1223–1245.